J. Phys. B: At. Mol. Opt. Phys. 27 (1994) 137–153. Printed in the UK

A study of electron capture and excitation processes in collisions of multiply charged ions with lithium atoms

J Schweinzer†, D Wutte‡ and H P Winter‡

† Max Planck Institut für Plasmaphysik, D-85748 Garching, Federal Republic of Germany
‡ Institut für Allgemeine Physik, Technische Universität Wien, Wiedner Hauptstrasse 8-10, A-1040 Wien, Austria

Received 6 August 1993, in final form 1 October 1993

Abstract. The atomic-orbital close-coupling method (AO-CC) has been employed in calculations of electron capture and target excitation in collisions of fully stripped ions A^{q+} ($q = 2-6$) with Li(ns, p) atoms ($n = 2, 3$) at low and intermediate energies. Total and state selective single electron capture (SEC) cross sections have been determined. Data for SEC into nl sub-levels of the projectile have been used to calculate the related line emission cross sections, which are compared with available experimental and theoretical data. In addition cross sections for various target excitation processes, in particular the Li(2s–2p) resonance transition are presented.

The scaling properties of the total SEC and target excitation cross sections are investigated, and their implication for lithium beam edge plasma spectroscopy is being discussed. For completion, scaling relations for ionization are also given.

1. Introduction

Inelastic transitions in collisions of multiply charged ions with lithium atoms in the ground state as well as in excited states are not only of fundamental interest, but of considerable importance for diagnostics of magnetically confined fusion plasmas by means of Li beam spectroscopy (Schweinzer *et al* 1992a, b). Injection of a beam of fast (1–10 keV amu^{-1}) neutral lithium atoms into a tokamak plasma has been shown to provide a wide range of diagnostic information. By analysing the line-radiation following collisions of Li atoms with plasma particles, properties of the plasma edge, such as the electron density (McCormick *et al* 1985, Schweinzer *et al* 1992b, Aumayr *et al* 1992), and the densities (Schorn *et al* 1991) and temperatures (Schorn *et al* 1992) of impurity ions can be determined.

Measuring electron densities (lithium impact excitation spectroscopy, Li-IXS) is based on the detection of the Li(2s–2p) resonance line at 670.8 nm, which becomes excited by collisions with the plasma particles. SEC from Li into highly excited states of impurity ions results in their characteristic lines radiation, in particular in the visible region, which provides most convenient experimental conditions (lithium charge exchange spectroscopy/Li-CXS) for detecting these plasma impurities. The advantages of injecting Li atoms instead of a hydrogen diagnostic beam have been discussed extensively by Winter (1982).

Evaluation of the diagnostic raw data relies on modelling the attenuation of the Li($n = 2, 3$) states beam fractions along the direction of injection (Schorn *et al* 1991,

0953-4075/94/010137+17$07.50

Schweinzer *et al* 1992b). Therefore, the success of these methods is strongly connected to the availability of reliable data on reaction cross sections for collisions of lithium atoms with all plasma particles such as electrons, protons and multiply charged impurity ions. Recently, a pertinent atomic data base which contains evaluated experimental and theoretical cross sections (Wutte *et al* 1993) has been established. All collision processes of electrons and protons with Li atoms relevant for diagnostic purposes have been considered in a wide energy range to describe the interaction of the injected beam with a clean plasma. However, in the plasma edge the fraction of impurity ions is certainly non-negligible and has also to be taken into account for a more accurate evaluation of diagnostic data (Schweinzer *et al* 1992a).

Total cross sections for SEC measured by different experimental groups in the particularly interesting energy range 1–10 keV amu^{-1} exist only for the He^{2+}–Li(2s) collision system (Gieler *et al* 1993b and references therein). So far, for higher charged projectiles, extensive quantitative measurements of line emission cross sections related to SEC from Li(2s) have been made so far for C^{4+} (Dijkkamp *et al* 1984) and for C^{6+}, N^{6+}, O^{6+} and Ne^{q+} (q=6–9) (Wolfrum *et al* 1992). Theoretical investigations of SEC into multicharged ions A^{q+} from Li(2s) employed either the semiclassical close coupling approach for He^{2+} (Fritsch and Lin 1983, Ermolaev *et al* 1987a, Sato and Kimura 1983) and for Be^{4+} (Fritsch and Lin 1984a), or the classical trajectory Monte Carlo (CTMC) method for Be^{4+} and B^{5+} (Hoekstra *et al* 1993) and for C^{6+} and O^{8+} (Olson *et al* 1992).

Whereas theoretical and experimental SEC data can be found for different projectiles, Li-target excitation by multiply charged ions has been investigated only for the case of He^{2+}–Li both theoretically (Ermolaev *et al* 1987b) and experimentally (Kadota *et al* 1982). Furthermore, no general scaling relations for low impact energies exist (Fritsch and Schartner 1987). Therefore, we performed large scale AO close-coupling calculations (AO-CC) for a variety of collision systems, involving fully stripped (charge state q equal to nuclear charge Z) ions A^{q+} (q=2–6) and lithium atoms in their ground and some excited states. In the plasma edge, incompletely stripped impurities are generally more abundant than fully stripped ones, but we have shown earlier (Wolfrum *et al* 1992) that for the application with Li-CXS the most relevant emission cross sections do mainly depend on the ion charge. Consequently the present calculations for fully stripped ions are also of interest for incompletely stripped impurities with equal q values.

The plan of the paper is as follows. In section 2 we provide some special aspects of the theoretical AO-CC method. Presentation of the results is given in section 3, where sections 3.1, 3.2 and 3.3 will deal with computed cross sections and their scaling properties for SEC, emission of characteristic radiation following SEC, and for target excitation processes, respectively. All atomic data are presented from the viewpoint of application to the lithium beam diagnostic. In section 3.4 we evaluate available atomic data for ionization of Li(2s). Finally, the main results are summarized.

2. Theoretical method

The well known semiclassical approach of expanding the total electron scattering wavefunction into target- and projectile-centred travelling atomic orbitals (AO), and solving the time-dependent Schrödinger equation in this truncated Hilbert space has been applied following Nielsen *et al* (1990).

The Fourier transform method (Shakeshaft 1975) has been used to evaluate two-centre matrix elements. It reduces a complicated three-dimensional integral to a sum of one-dimensional integrals over a finite range. The algebraic rules of Shakeshaft's formalism to produce the integrand structure are well suited for implementation in a symbolic manner to a computer code, as has been shown by Hansen (1990). The number of terms, however, when applying this formalism in its geometrically independent form, increases dramatically with n and l quantum numbers of the involved states, leading to extremely large requirements of computer memory. Therefore, additional procedures have been introduced to produce the most compact possible symbolic representation of the integrand for a chosen collision geometry. In this way, all presented calculations have been performed in the so-called collision system (Nielsen *et al* 1990). The projectile centred part of the basis is taken as exact q hydrogen-like states building complete shells with principal quantum numbers up to $n=8$.

In all calculations the $n=2, 3$ principal shells of Li have been included as the target centred part of the basis, except where otherwise stated. The interaction between the $Li^+(1s^2)$ core and the 'active' electron is described by a model potential of Rapp and Chang (1972). The radial parts of the corresponding eigenstates are expressed by sums of Slater-type orbitals. All other target-centred states are approximated by effective charge-hydrogenic states (Gieler *et al* 1993b). One-centre couplings between projectile states induced by the electric field of the Li^+ core are calculated by assuming a pure Coulomb interaction potential.

No pseudostates are included in the basis sets. Rather, a conventional AO expansion is used. For our lowest impact energy of 1 keV amu^{-1}, no inclusion of relaxed atomic orbitals of the united atom (UA) is needed, as has been demonstrated by Schweinzer and Winter (1990) for even smaller impact energies in the case of He^{2+}–Li(2s) collisions. Furthermore, for collision systems with increasing projectile charge, the inclusion of UA orbitals becomes increasingly redundant, at least if included at the projectile centre, since their respective overlaps with projectile orbitals become increasingly more important (Fritsch and Lin 1984b).

For capture and direct excitation in He^{2+}–Li(2s) collisions the importance of pseudostates representing transitions to the continuum in AO-CC calculations has been investigated by Ermolaev *et al* (1987a, b). They showed that for the SEC process a conventional AO expansion agrees remarkably well with a larger pseudostate expansion for $E<16$ keV amu^{-1}. Following Ermolaev (1987b), a stronger influence for the direct excitation process of such pseudostates should be expected. The neglecting of these pseudostates leads to an overestimation of the corresponding cross sections around the cross section maximum. By increasing the projectile charge, however, the coupling of excitation and continuum states should become weaker, since SEC dominates more and more the inelastic transitions in our energy range. Already from these considerations the chosen conventional AO expansion should be a sufficiently accurate representation for the main inelastic transitions.

3. Presentation of results and discussion

3.1. Total SEC cross sections

SEC from Li(nl) by multiply charged ions populates relatively high-n orbitals of the projectile. The quantum number n_0 of the dominantly populated shell can be derived

from our calculations by $n_0 = q + 1$ for Li(2s) and $n_0 = q + 2$ for Li(2p), respectively. The n-distribution in the projectile after SEC is narrowly peaked around n_0 at small impact energies and broadens with increasing energy, as to be expected. Since close coupling expansions are always limited to a few different principal shells, high impact energy corrections for SEC into higher n-shells as omitted in the expansion have been proposed (Ermolaev *et al* 1987a). However, such correction methods are inaccurate and have not been applied here. Instead our results for higher impact energies of up to 36 keV amu^{-1} are uncorrected total SEC cross sections, which were derived from AO-CC calculations involving principal shells with the largest quantum number $n_{max} = n_0 + 2$.

A scaling formula with respect to the initial state electron binding energy E_b (or principal quantum number $n = (2E_b)^{-1/2}$) and the charge of the fully stripped projectile has been derived by Janev (1991) for SEC from excited hydrogen atoms H(n) in a wide impact energy range. We introduce the same reduced impact energy and cross section by the relations (Janev 1991)

$$\tilde{E} = \frac{n^2 E}{\sqrt{q}} \qquad \tilde{\sigma} = \frac{\sigma}{n^4 q}. \tag{1}$$

This scaling has been verified until now mainly by CTMC calculations (Olson 1980) for A^{q+}-H(n) collisions. Such calculations use an initial momentum distribution of the active electron, corresponding to an equal population in n^2 of its (l, m) states. This initial condition is different from the case of a Li target where initial l states with specific angular momentum are involved. Furthermore, the non-integer quantum numbers n of Li states derived according to $n = (2E_b)^{-1/2}$ must be considered as an approximate measure only for the different initial charge cloud distributions, which are decisive for the SEC process. This is true especially for the low-lying states of Li. Therefore, we do neither expect that the general curve of Janev (1991) as proven valid for a hydrogen target may be used directly in the case of Li, nor that one single general curve could represent SEC from states with different angular momentum l. Reduced SEC cross sections for A^{q+}-Li(2s, 3s) collisions derived from AO-CC calculations are presented in figure 1. The scaling properties with respect to q are tested for a Li(2s) target and for six different charge states ($q = 1$–6) of the projectile. However, the scaling behaviour of the cross sections with respect to E_b (results for Li(3s)) is only checked for two projectiles ($q = 1, 2$). In addition to the AO results, the recommended cross sections (Wutte *et al* 1993) for H^+-Li(2s) collisions derived from experimental data of various groups are plotted in figure 1. All data points show a regular behaviour except results for (1) $q = 1$ at $\tilde{E} \leqslant 10$ keV amu^{-1} as is to be expected, because of the non-resonant SEC scenario, and for (2) $q = 5$, 6 at $\tilde{E} \geqslant 7$ keV amu^{-1}. The reason for the latter discrepancy is that only one higher excited projectile shell than the dominantly populated one has been included in these expansions ($n_{max} = n_0 + 1$), thus leading to an underestimation of the total cross section.The general curve (full curve in figure 1) represents a fit to all data points except the just mentioned ones with a five parametric analytic expression (cf appendix).

Total SEC cross sections derived from our AO calculations have been compared with other available experimental and theoretical data for A^{q+}-Li(2s) collisions in figure 2. Experimental results for He^{2+}-Li(2s) collisions (references cf figure 2) as well as theoretical results (AO-CC calculations of Fritsch and Lin 1984a, b, CTMC results of Hoekstra *et al* 1993) do not deviate by more than 10% from the general curve also drawn in figure 1, except for high impact energies where SEC from the K-shell of Li becomes

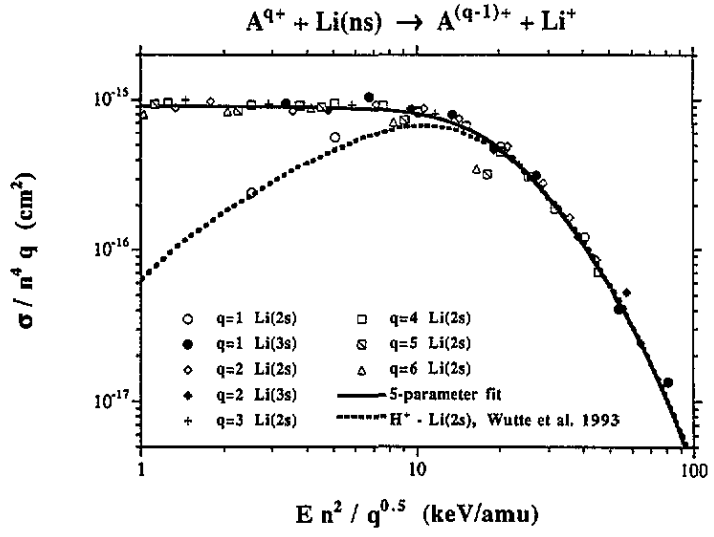

Figure 1. Calculated reduced total SEC cross sections for A^{q+}–Li(2s, 3s) collisions (open symbols) in comparison with recommended cross section for H^+–Li(2s) (broken curve), plotted against reduced impact energy. Full curve represents fit to data with analytic expression (cf appendix).

important. Finally, this general curve is supposed to predict total SEC cross sections for A^{q+}–Li(ns) collisions ($q \geq 2$; $n \geq 2$) in the range of reduced energy $\tilde{E} = 1$–80 keV amu^{-1}. For $\tilde{E} > 20$ keV the applicability of the general curve can be extended even to H^+–Li(ns) collisions.

In figure 3, computed reduced cross sections for A^{q+}–Li(np) ($q = 1$–6; $n = 2, 3$) collisions are compared with the experimental results for He^{2+}–Li(2p) (Gieler *et al* 1993b)

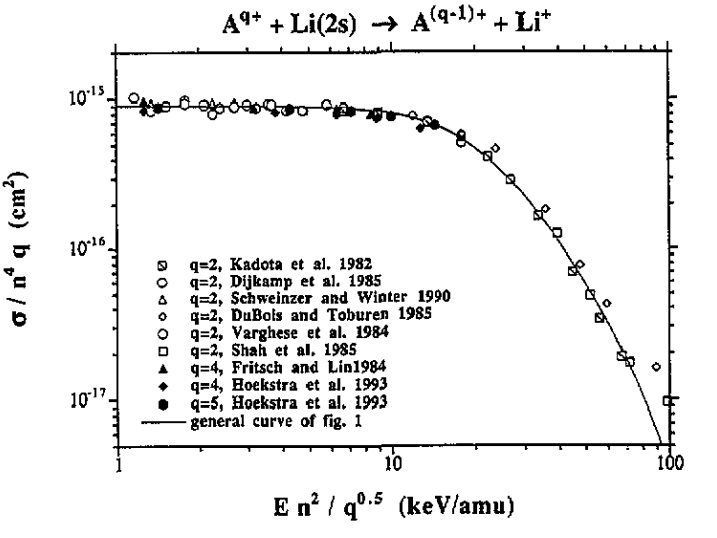

Figure 2. Experimental and theoretical reduced total SEC cross sections for A^{q+}–Li(2s) collisions (open symbols), plotted against reduced impact energy, in comparison with general curve of figure 1.

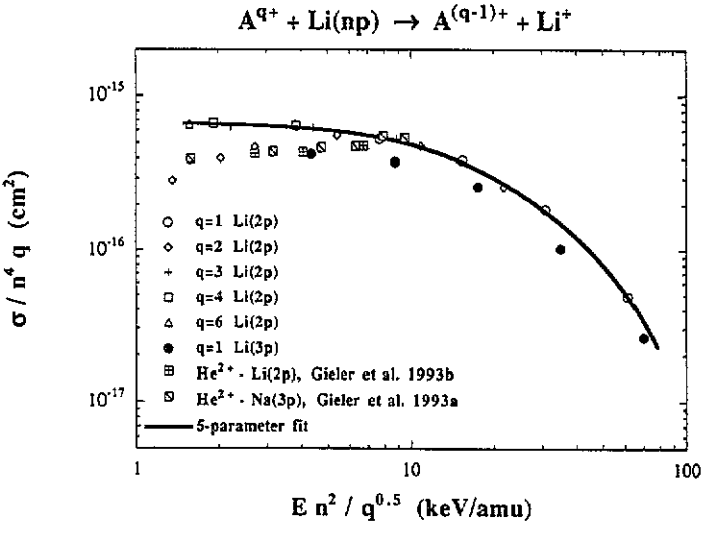

Figure 3. Calculated reduced total SEC cross sections for A^{q+}-Li(2p, 3p) collisions (open symbols), plotted against reduced impact energy, in comparison with experimental data for He^{2+}-Li(2p), Na(3p) collisions. Full curve represents fit to data with analytic expression (cf appendix).

and He^{2+}-Na(3p) (Gieler *et al* 1993a). All data points for A^{q+}-Li(2p) lie on a general curve, except those representing calculated and measured cross sections for He^{2+} projectiles at $\tilde{E} < 8$ keV amu^{-1}. Generally speaking, the behaviour at low impact energies of the total SEC cross section for multiply charged projectiles depends on the energetic position of the dominantly populated final shell with respect to the reaction window (Taulbjerg 1986). In the case of high q and/or high initial n the existence of favourably situated final states within the reaction window is always assured, leading to an almost velocity-independent behaviour of the total cross section at $\tilde{E} \leqslant 10$ keV amu^{-1} (cf figures 1–3).

3.2. Line emission cross sections

The $\Delta n = 1$ line emission cross sections are of fundamental interest for lithium beam activated charge-exchange spectroscopy (Li-CXS). Li-CXS is now an established method for the determination of impurity densities in the plasma edge, but further improvements and extension of the existing atomic data are necessary. So far, no line emission cross sections for collisions of plasma impurities heavier than He with excited Li atoms exist, while the importance of such atomic data for Li-CXS has been emphasized by Gieler *et al* (1993b).

We have constructed our theoretical emission cross sections by weighting the *nl*-selective cross sections from the AO-CC calculations with the corresponding branching ratios of specific $\Delta n = 1$ transitions. The branching rations have been calculated from transition probabilities for hydrogenic ions (e.g. Bethe and Salpeter 1957). A common feature of all $\Delta n = 1$ line emission cross sections is the dominant contribution of the *nl* sub-levels with the respectively highest angular momenta.

First, we compare our line emission cross sections with the experimental data of Wolfrum *et al* (1992) and the CMTC calculations of Olson *et al* (1992) for C^{6+} ions

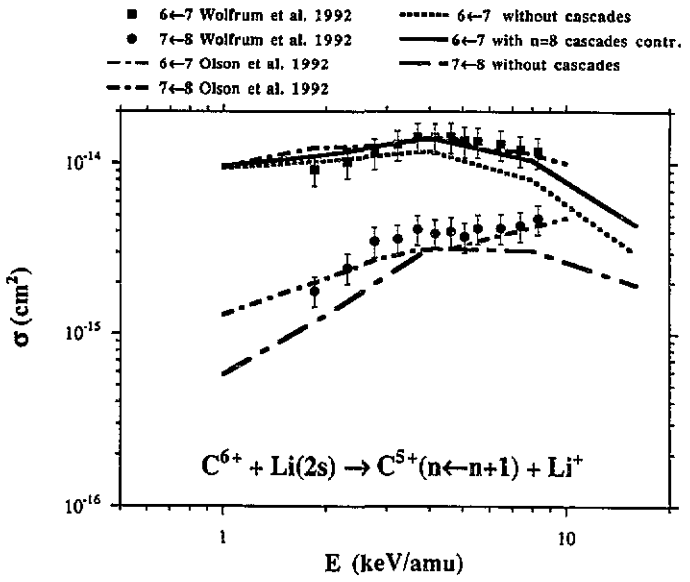

Figure 4. Calculated (lines) and experimental (full symbols) emission cross sections for $\Delta n = 1$ transitions in C^{6+}-Li(2s) collisions, plotted against impact energy.

colliding with Li(2s) (cf figure 4, including absolute error bars of 20% for the experimental data points). Excellent agreement is found for the 6←7 transition between both theories and the experimental values. Theoretical AO data for low impact energies overestimate the experimental data by 10% only.

For the 7←8 transition the AO calculation underestimates the experimental cross sections throughout the energy range. This deviation is not surprising, since no cascading contribution from $n \geqslant 9$ shells has been regarded. The effect of neglecting cascade contributions to an emission cross section has been demonstrated for the case of the 6←7 transition (cf figure 4, broken curve). Cascading from the $n = 8$ shell gives an important contribution to this total emission cross section, which reaches 30% at higher impact energies.

In figure 5 we compare line emission cross sections for He^{2+} and Be^{4+} projectiles with Li(2s) and Li(2p), respectively. In addition, experimental data for the He^{2+}-Li(2s) collision system of Aumayr *et al* (1989) and Hoekstra *et al* (1992) are presented. Perfect agreement with the results of Aumayr *et al* (1989) over the full energy range can be recognized. The data of Hoekstra *et al* (1992) are systematically lower, but agree, when considering their absolute error of 25%, still with our results.

All presented transitions become more probable for SEC from Li(2p) as compared to Li(2s) at impact energies below 10 keV amu^{-1}. This enhancement of emission cross sections for transitions like He II 3←4 (468.6 nm)and Be IV 6←7 (466.1 nm) exceeds a factor of ten at small impact energies, which is considerably more than one would expect from the enhancement of the corresponding total SEC cross sections. Such a strong enhancement will always occur for $\Delta n = n_0 \leftarrow n_0 + 1$ transitions (cf section 3.1 for definition of n_0) especially at small energies, because the $n_0 + 1$ final shell is populated dominantly for SEC from Li(2p) in contrast to Li(2s).

Although the fraction of Li(2p) usually does not exceed 15% in the probing beam (Schweinzer *et al* 1992b), line emission caused by SEC from Li(2p) contributes rather

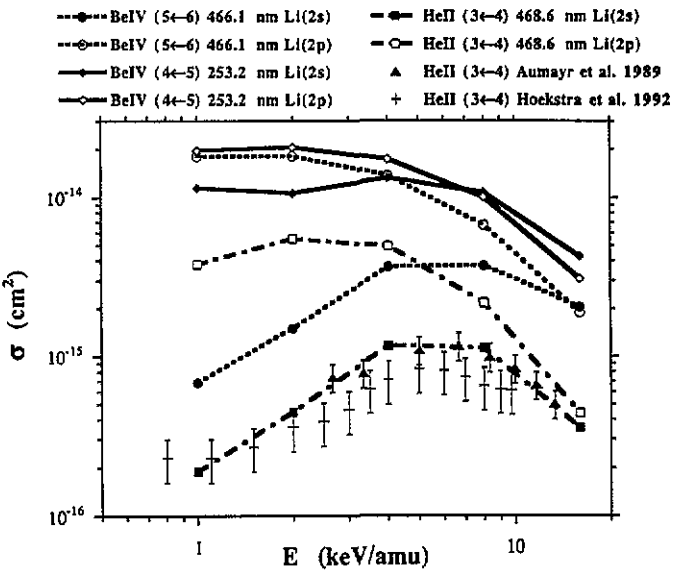

Figure 5. Calculated and experimental emission cross sections for $\Delta n = 1$ transitions in collisions of He^{2+} and Be^{4+} with Li(2s) (full symbols) and Li(2p) (open symbols), plotted against impact energy.

substantially to the total emitted characteristic radiation. Table 2 (cf appendix) summarizes all calculated line emission cross sections in units of 10^{-16} cm^2.

3.3. Target excitation processes

In general, single electron excitation processes in the adiabatic energy region involve cross sections much smaller than for SEC. At intermediate impact energies, however, cross sections for both processes are expected to involve the same order of magnitude.

3.3.1. Li(2s→2p) excitation. We have investigated the impact energy region of 1–100 keV amu^{-1}, where the main excitation process Li(2s–2p) (excitation energy ΔE= 1.85 eV) becomes the dominant inelastic transition. In particular the excitation process in He^{2+}–Li(2s) collisions has been chosen for an extensive investigation, because experimental data (Kadota *et al* 1982) as well as another detailed theoretical study (Ermolaev *et al* 1987b) are already available for comparison. The Li(2s–2p) excitation cross sections presented in figure 6 have been derived from close coupling calculations with different expansions, in order to deduce the strength of various couplings between different reaction channels especially at low impact energies ($E \leqslant 8$ keV amu^{-1}).

First, we discuss the low energy results, which besides their fundamental interest are particularly important for the Li-IXS diagnostic purpose. We start with a one-centre expansion (AO9, cf figure 6), including only states on the target centre. This calculation predicts large excitation cross sections, which even increase with decreasing impact energy ($E \leqslant 5$ keV amu^{-1}). This unexpected behaviour disappears when SEC channels are added to the basis (AO15, AO19, AO25 and AO29 in figure 6). Obviously, the strongly competing SEC channels are mainly responsible for the decline of the excitation cross section towards lower impact energies. At impact energies $E < 4$ keV amu^{-1} even weakly or almost not populated tight bound SEC channels of He^+ $n = (1, 2)$ show an amazing

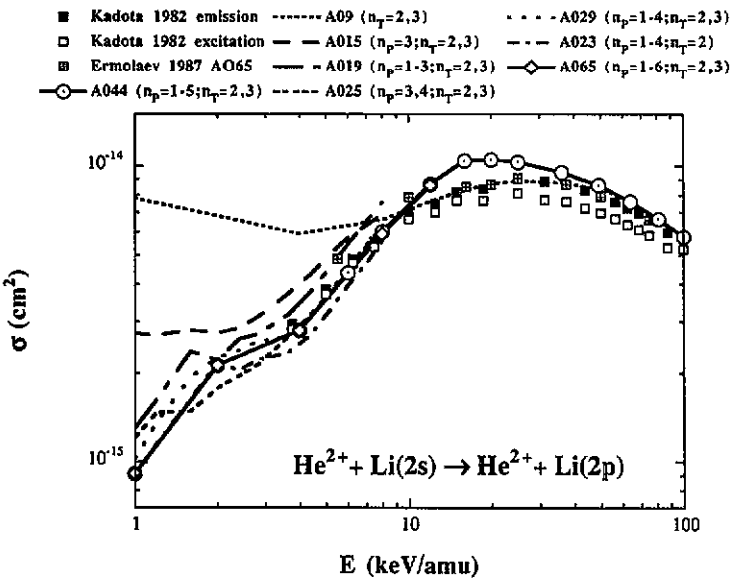

Figure 6. Results from AO-CC calculations with different expansions in comparison with experimental and theoretical cross sections for the Li(2s-2p) excitation process in He^{2+}–Li(2s) collisions, plotted against impact energy.

influence on the excitation process (compare AO15 with AO19, and AO25 with AO29, respectively). However, inclusion of still further SEC channels (compare AO29, AO44 and AO65 in figure 6) does not alter results considerably. The results of the AO44 calculation have already perfectly converged, as can be seen by comparing them with AO65. The quality of the cross sections derived from the AO44 calculation is further demonstrated by the excellent agreement with the experimental data points of Kadota *et al* (1982). Furthermore, one-centre couplings between Li($n=2$) and Li($n=3$) states seem to be less important for the excitation process than coupling of Li($n=2$) to the SEC channels, as can be deduced by considering the comparatively small differences between results of AO29 and AO23, where the Li($n=3$) shell has been omitted in the latter expansion.

A general rule for choosing the appropriate SEC channels for calculating excitation cross sections within the AO-CC approach at low impact energies can be deduced from the above findings. It immediately follows that the projectile-centred part of the basis should include at least final states, which are dominant SEC channels in collisions with both the initial as well as the final target states of the considered excitation process.

The results of different AO-CC calculations at energies $E > 8$ keV amu^{-1}, especially the comparison of pure bound states with pseudostate expansions as well as the deviations of theoretical results from the measured excitation cross section of Kadota *et al* (1982) has been discussed in detail by Ermolaev *et al* (1987a, b). Experimental results are better reproduced around the cross section maximum (in the region $12 \leqslant E \leqslant 64$ keV amu^{-1}) by the simple one-centre expansion AO9, than by the much larger AO44 calculation which includes all relevant SEC channels. This striking effect has also been found by Ermolaev *et al* (1987a, b) and is due to the lack of coupling between SEC channels with the continuum states representing ionization. We therefore take the results of the AO9 calculation in the vicinity of the maximum to represent the excitation cross section in this collision system. For higher charged projectiles, however, this effect

is much less pronounced and vanishes already completely in the case of C^{6+}-Li(2s) collisions.

Janev and Presnyakov (1980) have derived a general expression for excitation cross sections on the basis of a three-state close-coupling dipole approximation introducing reduced cross sections σ/q and impact energies E/q.

The validity of this scaling has been restricted by Fritsch and Schartner (1987) to energies $E/q > 15$ keV amu^{-1} via large scale AO-CC calculations for A^{q+}-H(1s) collisions. Furthermore, the general curves from both investigations deviate from each other (for further discussions, cf Fritsch and Schartner 1987).

We compare our theoretical cross sections for the Li(2s-2p) excitation in A^{q+}-Li(2s) ($q = 2, 4, 6$) collisions with the experimental data of Aumayr *et al* (1984) for H^+-Li(2s) and with the respective reduced electron excitation cross sections (cf Wutte *et al* 1993).

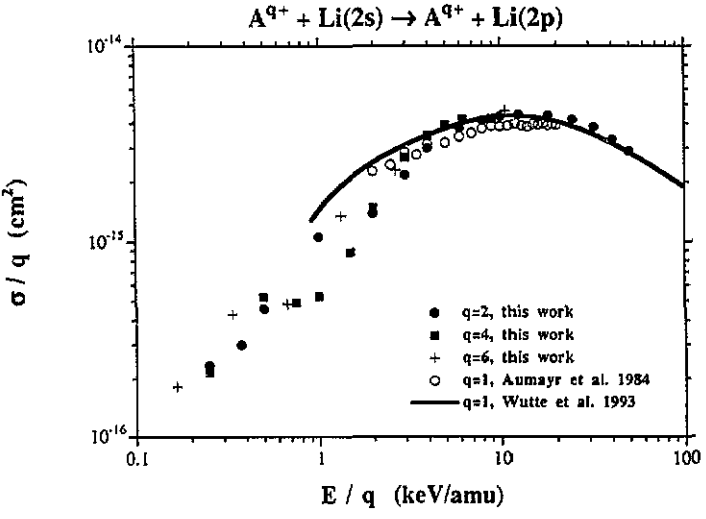

Figure 7. Calculated and experimental reduced cross sections for Li(2s-2p) excitation in A^{q+}-Li(2s) collisions, plotted against reduced impact energy.

As can be seen in figure 7, theoretical data points for different charged projectiles ($q = 1$-6) lie approximately on the full curve representing the reduced electron excitation cross section for $E/q \geq 4$ keV amu^{-1}. The experimental points tend to stay by 10% below the full curve. The breakdown of this scaling for lower impact energies coincides with the beginning of strong competitive coupling between SEC and excitation channels (compare figure 6).

The confirmed cross section scaling for higher impact energies is not very helpful for Li-IXS, since even for high injection energies like $E_{beam} = 70$ keV the application is excluded by the above requirement $E/2 \geq 4$ keV amu^{-1}. Therefore, the low energy part of figure 7 (with additional results from AO-CC calculations for $q = 3, 5$) is again presented without any scaling attempt in figure 8. For impact energies $E \leq 4$ keV amu^{-1}, Li(2s-2p) excitation in A^{q+}-Li(2s) collisions is less probable than in H^+-Li(2s) collisions. This is again due to the increased density of SEC channels for multiply charged projectiles in comparison to protons. Charge-averaged cross sections have been calculated at $E = 1, 2, 4, 8, 16$ keV amu^{-1} (the numerical values are given in table 3 of the appendix) and linearly interpolated (figure 8). Although the deviation from this charge-averaged curve reaches ±30% at $E = 1$ and 4 keV amu^{-1}, it represents a 'universal' cross

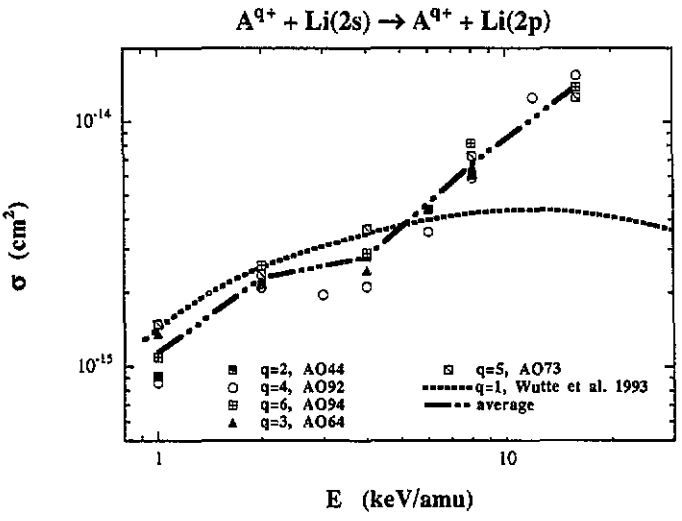

Figure 8. Calculated cross sections for Li(2s–2p) excitation in collisions of A^{q+}–Li(2s) (q = 1–6, symbols) in comparison with q-averaged cross section (broken curve) and the recommended cross section for H^+–Li(2s) collisions, plotted against impact energy.

section which can be conveniently implemented into plasma edge Li-IXS diagnostic codes. Considering in addition, that only estimates of the distributions of impurity ions in different ionization stages in the plasma edge (cf Schweinzer *et al* 1992a, b) are possible, the charge-averaged curve can be considered as appropriate for this purpose.

3.3.2. Li(2p→3s, p, d) excitation. Transitions from Li(2p) to Li(3s), Li(3p) and Li(3d) involve excitation energies of 1.53, 1.98 and 2.01 eV, respectively. These energies are rather similar to the already discussed case of Li(2s–2p) excitation. However, converged results of AO-CC calculations for low impact energies can only be expected, if the dominant channel for SEC from Li(3*l*) is represented in the expansion (cf section 3.3.1). This leads to an extremely large number of basis states, especially for higher q values of the projectile, and conseqently to rather CPU-time consuming computations. Therefore, we have calculated the cross sections for these excitation processes only for the He^{2+} case. In figure 9 three different AO-CC calculations are compared. The unsatisfactory convergence at low impact energies between the AO44 (He II n = 1–5) and AO65 (He II n = 1–6) results confirms our findings from section 3.3.1, concerning the necessary minimal number of projectile-centred basis states. Increasing the impact energy leads to better convergence between these two different expansions. Finally, at 16 keV amu^{-1}, derivation of the same cross sections from a pure one-centre expansion AO14 (Li(n= 2, 3, 4p, 4d)) coincides with results from the larger expansions.

The scaling properties with respect to the charge of the projectile have been investigated by comparing AO-CC results for He^{2+}, Li^{3+} and Be^{4+}, where the dominant shell for SEC from Li(3*l*) has been omitted in the corresponding expansions. Nevertheless, we found an approximate scaling of $\sigma(E)/q$ to hold at energies $E \geqslant 4$ keV amu^{-1} and $E \geqslant 2$ keV amu^{-1} for the Li(2p)→Li(3p, d) and for the Li(2p)→Li(3s) excitation processes, respectively. This scaling is different from that of section 3.3.1, because no reduced impact energy occurs now in the relation. The much stronger competitive target-centred couplings in the case of the Li(2p–3l) transition in comparison to the

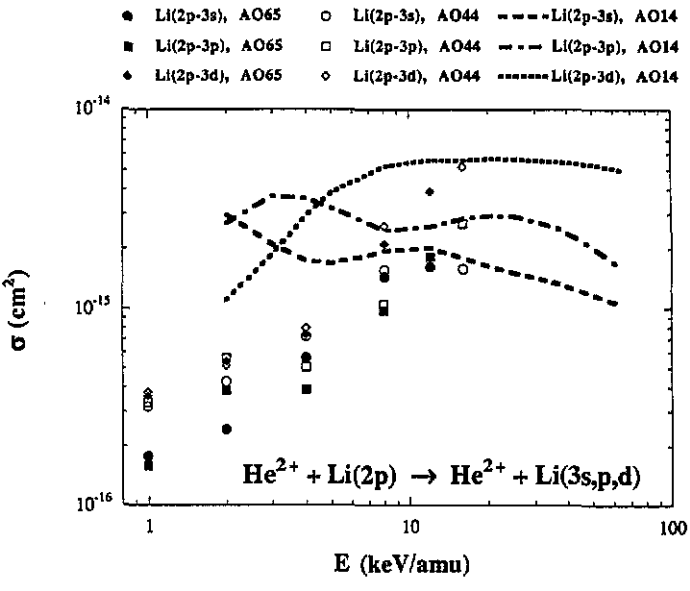

Figure 9. Calculated cross sections derived from AO-CC calculations with two-centre expansions (symbols) and a single one-centre expansion (curves) for the Li(2p–3s, p, d) excitation processes in He^{2+}–Li(2p) collisions, plotted against impact energy.

dominant excitation process Li(2s–2p), might explain this different scaling behaviour. For lower impact energies no significant enhancement of the cross section with increasing q has been observed.

Therefore, we suggest for the Li–IXS diagnostic purpose to take the results for the He^{2+} projectile (cf table 4) and

(i) to apply the above scaling relation at high impact energies and

(ii) to use them as a charge-independent cross sections for the Li(2p–3l) excitation in collisions with multiply charged ions at lower impact energies.

3.3.3. Li(2s→3s, p, d) excitation. For these excitation processes only small cross sections are expected, because of the rather large excitation energies of 3.37, 3.83 and 3.86 eV for Li(2s–3s), Li(2s–3p) and Li(2s–3d) transitions, respectively. In general, it is difficult to derive cross sections from AO-CC calculations, for inelastic transitions which are by two orders less probable than the dominant ones since many different channels interact with each other. Ermolaev *et al* (1987) have calculated the Li(2s–3d) excitation cross sections by comparing different expansions including one also with continuum states. The influence of pseudostates has turned out to be much stronger than in the case for the dominant excitation channel. Although we neglect such states in our calculation, results of our AO-CC are presented and should be considered as a first estimate.

In figure 10 again two AO-CC calculations are compared with the only experimental results of Kadota *et al* (1982) for He^{2+}–Li(2s) collisions. The convergence between a pure one-centre expansion AO14 (Li($n=2,3;4p,4d$)) and the AO65 results can be observed only for very high impact energies. Around the maximum of the Li(2s–3d) excitation cross section our results overestimate the experimental data by almost a factor of two. Below 12 keV amu^{-1}, however, we believe that our results give a relatively

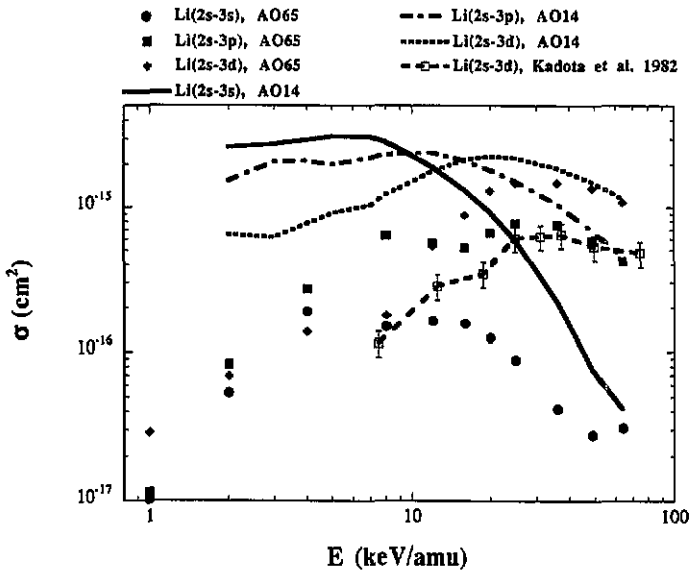

Figure 10. Calculated cross sections derived from AO-CC calculations comparing a two-centre expansion (symbols) with a one-centre expansion (curves) for the Li(2p–3s, p, d) excitation processes in He^{2+}–Li(2p) collisions, together with experimental cross sections for the Li(2p–3d) excitation, plotted against impact energy.

better estimate for the cross section, because the influence of ionization should be less important. For this energy region we suggest for the Li-IXS purpose based on the experience gained for other excitation processes (cf sections 3.3.1 and 3.3.2), to apply the results of the AO65 AO-CC (cf table 3) again as a charge-independent cross section for collision of all multiply charged ions.

3.3.4. Li(3s→3p, d) and Li(3p→3d) excitation. Excitation processes between Li(*nl*) states of the same principal shell involve small excitation energies only. Therefore, such transitions are determined by large impact parameter ($b > 20a_0$) collisions, where actually no competition by SEC has to be taken into account throughout the complete impact energy range (1–100 keV). The scaling behaviour has been derived from one-centre AO-CC calculations for H^+ and He^{2+} colliding wth Li(3*l*), given a reasonable $\sigma(E/q)/q$ cross section scaling.

3.4. Ionization of Li

In order to obtain scaling relations for all inelastic transitions relevant for Li-IXS, we have also analysed available atomic data for ionization of H(*n*) and Li(2s) colliding with multiply charged ions. Olson (1980) has verified the scaling relation of equation (1) for ionization with respect to different binding energies of the electron in its initial state in collisions of A^{q+} ($q = 1, 2, 5, 10$) with H(*n*) ($n = 1$–25), by using the CTMC

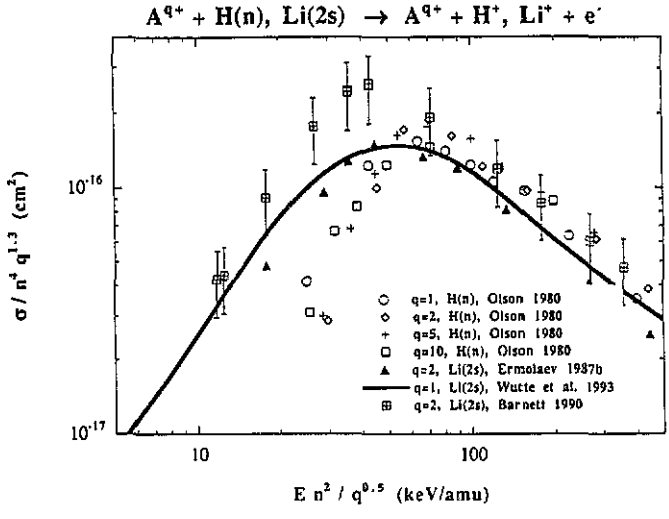

Figure 11. CTMC results (Olson 1980) for ionization of H(1s) by multiply charged ions, and experimental (Wutte *et al* 1993, Barnett 1990) and theoretical (Ermolaev 1987b) reduced cross sections for the ionization of Li(2s) in collisions with A^{q+}, plotted against reduced impact energy.

method. No scaling with respect to q has been proposed in this study for the lower energy part. With a slightly stronger q-dependence (cf equation (2)) for the reduced cross section than in the case of SEC (cf section (3.1)), we could approximately retrace these CTMC results (cf figure 11) in our energy region.

$$\tilde{E}=\frac{n^2E}{\sqrt{q}} \qquad \tilde{\sigma}=\frac{\sigma}{n^4\cdot q^{1.3}}. \tag{2}$$

The scaling relation of equation (2) has been optimized for $\tilde{E}<100$ keV amu^{-1}. Two recommended curves for ionization of Li(2s) by H^+ (Wutte *et al* 1993) and He^{2+} (Barnett 1990) as well as the AO-CC results for He^{2+} (Ermolaev *et al* 1987b) have been added to figure 11. Whereas data points for $\tilde{E}>100$ keV amu^{-1} lie roughly on the general curve, the situation for lower reduced energies looks less satisfactorily. The recommended curve of Barnett (1990) is based on measurements of Shah *et al* (1985) with an absolute error of ±20% and has not been confirmed by quantal calculations (e.g. Ermolaev *et al* 1987b).

The factor of 1.7 between the two recommended curves of figure 11 representing ionization of Li(2s) in collisions with H^+ and He^{2+}, respectively, points to a still stronger q-dependency (e.g. q^2) of the reduced cross section. However we suggest to apply the proposed scaling relation (equation (2)) especially for higher q values, thus giving more confidence to the CTMC results of different highly charged projectiles than to one single measurement for He^{2+}.

4. Summary and concluding remark

We have presented a study, urged by the need for atomic data for lithium beam activated edge plasma spectroscopy, dealing with both SEC from Li(ns, np) ($n\geqslant 3$) into multiply

charged ions and with excitation processes between all Li(nl) ($n \leqslant 3$) levels in the energy range 1–100 keV amu^{-1}. General curves of highly accurate reduced cross sections have been established for the dominant inelastic transitions. Approximate cross section scaling relations and estimates of cross sections for the weaker inelastic transitions have also been given. In addition, emission cross sections have been calculated for direct application to Li–CXS. The presented atomic data have been generated with a variety of AO-CC calculations with different expansions of up to 94 fully coupled bound states.

A scaling relation for SEC from Li(nl) has been proven valid to a high degree with respect to q. On the other hand, deviations by up to 40% from an established scaling for the same process with respect to the binding energies of the active electron on Li(nl) target states with different angular momenta l have been found. Therefore, cross sections for SEC from states with different initial angular momenta do not fit exactly on a single general curve.

The competitive influence of SEC channels to target excitation processes in slow collisions has been investigated more extensively by comparing different AO expansions. Inclusion of basis states dominantly populated by SEC from both the initial and the final levels of the considered excitation process into an AO expansion seems to be necessary to obtain reasonable cross sections for such slow collisions. At impact energies where strong coupling to the SEC channels considerably influences the excitation process, in first approximation almost no q-dependence of the corresponding cross section has been found. The excitation process becomes decoupled from SEC at impact energies according to the excitation energy ΔE and exhibits then an ordered behaviour with respect to changing q.

In general, the agreement between the computed results and experimental as well as theoretical data of other authors is very good for the main inelastic transitions. For cases where our AO-CC calculations deliver less accurate results, inclusion of pseudostates representing ionization channels would certainly further improve our results. Although this would be quite feasible, such large computations will be performed only if test calculations with the Li-IXS data evaluation codes containing the presented atomic data would show a high sensitivity to the mentioned uncertainties of the weaker inelastic transitions.

Appendix

The analytical al curves (cf figures 1–3 and section 3.1 for range of validity) of reduced cross sections for SEC from Li(2s, 3s) and Li(2p, 3p) plotted against $\tilde{E}$ (keV amu^{-1}), respectively, are given in equation (3), corresponding coefficients to be found in table 1.

$$\tilde{\sigma}(\mathrm{cm}^2) = A_1 \frac{(1 - \mathrm{e}^{-\tilde{E}A_2/A_3})}{\tilde{E}^{A_2} + A_4 \tilde{E}^{A_5}}. \tag{A1}$$

Table 1. Coefficients for analytical expression of equation (3).

	A1	A2	A3	A4	A5
Li(2s, 3s)	7.513×10^{-10}	3.14	8.307×10^{5}	1.41×10^{-4}	6.062
Li(2p, 3p)	4.513×10^{-10}	3.204	6.738×10^{5}	6.828×10^{-3}	4.933

Table 2. Calculated emission cross sections in units of 10^{-16} cm^2 for $\Delta n = 1$ transitions in collisions of He^{2+}, Be^{4+} and C^{6+} with Li(2s, 2p) for five impact energies E.

E (keV amu^{-1})	Li(2s) He II 3←4	Li(2p) He II 3←4	Li(2s) Be IV 4←5	Li(2p) Be IV 4←5	Li(2s) Be IV 5←6	Li(2p) Be IV 5←6	Li(2s) C VI 6←7	Li(2s) C VI 7←8
1	1.9	37.8	115.0	197.0	6.85	181.0	96.5	5.79
2	4.47	54.8	107.0	206.0	15.00	182.0	111.0	12.8
4	11.6	49.2	133.0	174.0	36.40	138.0	140.0	31.8
8	11.2	21.7	108.0	101.0	37.10	67.1	104.0	30.8
16	3.54	–	42.5	–	20.40	–	43.9	19.4

Table 3. Charge averaged cross sections in cm^2 for Li(2s–2p) excitation derived from AO-CC calculations, for A^{q+}-Li(2s) ($q = 2$-6) collisions. The deviation from the mean values at each impact energy E is also given in addition.

E (keV amu^{-1})	Li(2s–2p)
1	1.14e−15 ± 30%
2	2.28e−15 ± 10%
4	2.77e−15 ± 30%
8	6.70e−15 ± 20%
16	1.39e−14 ± 10%

Table 4. Excitation cross sections in units of 10^{-16} cm^2 for collisions of He^{2+} with Li(2s, 2p), derived from AO65 close coupling calculations (cf text).

E (keV amu^{-1})	Li(2s–3s)	Li(2s–3p)	Li(2s–3d)	Li(2p–3s)	Li(2p–3p)	Li(2p–3d)
1	0.103	0.115	0.291	1.80	1.59	3.6
2	0.54	0.835	0.697	2.44	3.86	5.4
4	1.89	2.70	1.38	5.65	3.88	7.4
8	1.49	6.36	1.77	15.0	9.80	21.1
12	1.62	5.63	5.33	16.3	18.2	39.1

References

Aumayr F, Fehringer M and Winter H P 1984 *J. Phys. B: At. Mol. Phys.* **17** 4185

Aumayr F, Schweinzer J and Winter H P 1989 *J. Phys. B: At. Mol. Opt. Phys.* **22** 1027

Aumayr F, Schorn R P, Pöckl M, Schweinzer J, Wolfrum E, McCormick K, Hintz E and Winter H P 1992 *J. Nucl. Mat.* **196–198** 928

Barnett C F 1990 *Atomic Data for Fusion* vol 1 (Oak Ridge, USA: Controlled Fusion Data Centre, Oak Ridge National Laboratory)

Bethe H A and Salpeter E E 1957 *Quantum Mechanics of One- and Two-Electron Atoms* (Berlin: Springer)

DuBois F D and Toburen L H *Phys. Rev.* A **31** 3603

Dijkkamp D, Brazuk A, Drentje A G, deHeer F J and Winter H P 1984 *J. Phys. B: At. Mol. Phys.* **17** 4371

Dijkkamp D, Boellard A and deHeer F J 1985 *Nucl. Instrum. Methods* B **9** 377

Ermolaev A M, Hewitt R N and McDowell M R C 1987a *J. Phys. B: At. Mol. Phys.* **20** 3125

Ermolaev A M, Hewitt R N, Shingal R and McDowell M R C 1987b *J. Phys. B: At. Mol. Phys.* **20** 4507

Fritsch W and Lin C D 1983 *J. Phys. B: At. Mol. Phys.* **16** 1595

—— 1984a *J. Phys. B: At. Mol. Phys.* **17** 3271

—— 1984b *Phys. Rev.* A**29** 3039

Fritsch W and Schartner K H 1987 *Phys. Lett.* **126A** 17

Gieler M, Aumayr F, Schweinzer J, Koppensteiner W, Husinsky W, Winter H P, Lozhkin D and Hansen J P 1993a *J. Phys. B: At. Mol. Opt. Phys.* **26** 2137

Gieler M, Aumayr F, Weber M, Winter H P and Schweinzer J 1993b *J. Phys. B: At. Mol. Opt. Phys.* **26** 2153

Hansen J P 1990 *Comput. Phys. Commun.* **58** 217

Hoekstra R, Olson R E, Folkerts H O, Wolfrum E, Pascale J, de Heer F J, Morgenstern R and Winter H P 1993 *J. Phys. B: At. Mol. Opt. Phys.* **26** 2029

Hoekstra R, Wolfrum E, Beijers J P M, de Heer F J, Winter H P and Morgenstern R 1992 *J. Phys. B: At. Mol. Opt. Phys.* **25** 2587

Kadota K, Dijkamp D, van der Woude R L, Yan P G, deHeer F J 1982 *J. Phys. B: At. Mol. Phys.* **15** 3297

Janev R K 1991 *Phys. Lett.* **160A** 67

Janev R K and Presnyakov L P 1980 *J. Phys. B: At. Mol. Phys* **13** 4233

McCormick K and the ASDEX team 1985 *Rev. Sci. Instrum.* **56** 1063

Nielsen S E, Hansen J P and Dubois A 1990 *J. Phys. B: At. Mol. Opt. Phys.* **23** 2595

Olson R E 1980 *J. Phys. B: At. Mol. Phys.* **13** 483

Olson R E, Pascale J and Hoekstra R 1992 *J. Phys. B: At. Mol. Opt. Phys.* **25** 4241

Rapp D and Chang C M 1972 *J. Chem. Phys.* **57** 4283

Sato H and Kimura M 1983 *Phys. Lett.* **96A** 286

Schorn R P, Hintz E, Rusbüldt D, Aumayr F, Schneider M, Unterreiter E and Winter H P 1991 *Appl. Phys.* B **52** 71

Schorn R P, Wolfrum E, Aumayr Fm Hintz E, Rusbüldt D and Winter H P 1992 *Nucl. Fusion* **32** 351

Schweinzer J, McCormick K, Fiedler S, Aumayr F, Pöckl M and Winter H P 1992a *Proc. 19th EPS Conference on Controlled Fusion and Plasma Physics (Innsbruck)* Contributed paper

Schweinzer J and Winter H P 1990 *J. Phys. B: At. Mol. Opt. Phys.* **23** 3881

Schweinzer J, Wolfrum E, Aumayr F, Pöckl M, Winter H P, Schorn R P, Hintz E, Unterreiter A 1992b *Plasma Phys. Controlled Fusion* **34** 1173

Shah M B, Elliott D S and Gilbody H B 1985 *J. Phys. B: At. Mol. Phys.* **18** 4245

Shakeshaft R, 1975 *J. Phys. B: At. Mol. Phys.* **8** L134

Taulbjerg K, 1986 *J. Phys. B: At. Mol. Phys.* **19** L367

Varghese S L, Waggoner W and Cocke C L 1984 *Phys. Rev.* A **29** 2453

Winter H P 1982 *Comment. At. Mol. Phys.* **12** 165

Wolfrum E, Hoekstra R, de Heer F J, Morgenstern R and Winter H P 1992 *J. Phys. B: At. Mol. Opt. Phys.* **25** 2697

Wutte D, Janev R K, Schneider M, Smith J J, Aumayr F, Schweinzer J and Winter H P 1993 *Report IAEA-INDC-NDS 267 IAEA* in preparation